COMPUTER SCIENCES

Computer-Assisted Liver-Mass Estimation from Gamma-Camera Images

Edward A. Eikman, Gregory A. Mack, Vijay K. Jain, and Joseph A. Madden

University of South Florida and Veterans Administration Hospital, Tampa, Florida

We have devised a computer-assisted method for objective estimation of liver mass from the right lateral projection of radiocolloid images of the liver. Gamma-camera images were digitized, preprocessed, and stored in computer memory. The definition of liver for area measurement was adaptively determined by means of a Laplacian operator that measures change in radioactivity slope associated with the liver margin. Individual thresholds were calculated for each of 16 subregions. A liver-mass index was derived from a linear regression model correlating the area of the right lateral projection with liver weight at autopsy in 50 patients whose livers weighed between 0.8 to 3.0 Kg. The correlation coefficient found for this method was 0.83 using the equation: Liver Mass $[kg]$ = Area $[cm^2]/275$ $[kg/cm^2]$ − 0.215 $[kg]$. Liver-mass estimates using an alternative computer-assisted method or representative manual methods adapted for gamma-camera images showed lower correlation with liver weight at autopsy.

Several manual measurements extracted from radiocolloid liver images have been proposed as direct or indirect indices of liver mass (*1–3*). Rectilinear scans were used, but the methods are adaptable to the gamma camera. These adapted manual methods, however, are tedious and are potentially subject to several sources of error. We report a computer-assisted method for estimating liver mass from gamma-camera images that is more accurate than the adapted manual methods we have tested.

PATIENTS AND METHODS

Patients studied were referred to the Nuclear Medicine Service for radiocolloid imaging between September 1, 1973, and September 1, 1977. Images were stored in digital form, without selection, on magnetic disk. Images from 82 patients who subsequently died and had liver-weight measurements at autopsy were screened for inclusion in this study. Patients were excluded if the right lateral image was too large to fit into the gamma-camera field of view, if appreciable rib radioactivity was included in the images, or if ascites was evident as a ring of reduced radioactivity around the liver image. Patients with liver neoplasms were excluded if they died more than 30 days after imaging. If more than one liver-imaging study was performed, only the study performed closest to the date of death was included. Fifty male patients ranging in age from 33 to 82 years, mean age 52, remained. Autopsy diagnoses of the liver were categorized as: a) nonneoplastic

liver disease (n = 32), b) neoplastic liver disease (n = 3), or c) no recognized liver disease (n = 10).

Image production. Gamma images of the anterior, right lateral, and posterior projections of the liver were acquired 15–30 min after i.v. injection of 2–4 mCi of Tc-99m sulfur colloid. The patient remained supine throughout the study. A gamma camera* with a high-resolution parallel-hole collimator was used to construct a 400,000-count image of each projection, using a 20% window centered over the 140-keV photopeak. On each day of imaging, a 2-million-count image of a Tc-99m pool source was obtained to detect changes in uniformity and sensitivity of the detector and to provide an image-size reference. Images from the camera were photographed on 35-mm SF2 film†. Intensity settings were adjusted from day to day in order to preserve visual gray-scale resolution between the lightest and darkest portions of the images. Each image was recorded on a video tape recorder and replayed, if necessary, to correct errors in intensity settings.

Manual image tracings. A microfilm reader‡ was adjusted by means of the pool-source image to display full-sized images on a back-projection reading screen. The outline of the full-sized liver image was traced on translucent paper applied to the front of the screen in a darkened room. The liver margin was chosen at about half the distance from the faintest detectable edge activity and a subjective central activity plateau that is usually detectable within a few millimeters of the faintest edge. After initial comparison, in order to standardize the tracing method, observers made all measurements independently.

Computer definition of liver margins. The analog data from each image were converted into a 64 × 64 digital image matrix with a minicomputer. Image data were stored on disks or tape for later analysis.

Image noise beyond the spatial frequency limit of the gamma camera was reduced by applying a nine-point moving-average filter (4) with the following weights:

$$\begin{bmatrix} .08 & .08 & .08 \\ .08 & .36 & .08 \\ .08 & .08 & .08 \end{bmatrix}$$

An edge-shaping operator was applied to the filtered data to accentuate the boundaries. Each image pixel, f(x,y), was replaced with:

$$f(x,y) = \begin{cases} f(x,y) \left[\dfrac{f(x,y)}{T}\right]^4, & \text{for } f(x,y) < T \\ \\ T & , & \text{for } f(x,y) \geq T \end{cases}$$

where T is 25% of the maximum pixel count in the image, or 150, whichever is smaller.

A 25-point smoothed Laplacian operator was then applied:

$$\begin{bmatrix} 0 & -1 & -1 & -1 & 0 \\ -1 & 2 & 1 & 2 & -1 \\ -1 & 1 & 0 & 1 & -1 \\ -1 & 2 & 1 & 2 & -1 \\ 0 & -1 & -1 & -1 & 0 \end{bmatrix}$$

Each pixel was replaced by a summation over the nearest-neighbor pixels using these coefficients. This discrete Laplacian is analogous to the more familiar continuous domain expression:

$$\nabla^2 f(x,y) = \frac{\partial^2}{\partial x^2} f(x,y) + \frac{\partial^2}{\partial y^2} f(x,y).$$

The Laplacian operator gives a measure of the curvature with respect to the x-y plane for any point in the image. Maximum curvature occurs where the slope of radioactivity is changing most rapidly.

The resulting matrix was partitioned into sixteen 8 × 32 submatrices, and a maximum Laplacian was found for each row in each of the partitions (5). An adaptive count threshold was determined for each partition by computing the average of the pixel counts at the Laplacian maxima. All image points below the threshold for the partition were set to zero.

The image area was computed from the number of nonzero pixels and normalized to a reference area defined by the field of view.

Manual measurements. For each patient studied, the average of three separate determinations of the following manual measurements was recorded from the tracings of the liver:

1. *Manual anterior area (1).* The area of the image from the anterior projection was measured by manual planimetry.

2. *Manual right lateral area.* The area of the image from the right lateral projection was measured by manual planimetry.

3. *Manual geometric model (2).* The left lobe of the liver was sketched to approximate a paraboloid, and the right lobe to approximate an ellipsoid, according to the procedure in the reference cited. The base and height of the paraboloid, and the axes of the ellipsoid, were used to calculate an estimated volume of the liver using the published formula.

4. *Manual dimension A (3).* The height of the liver along the longitudinal axis from the dome of the liver to the inferior margin was used to approximate the dimension A, which was originally reported as a liver-size-related index of liver disease.
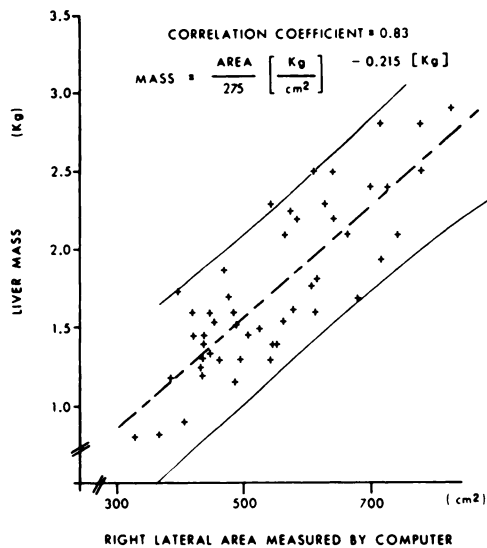
FIG. 1. Liver-mass index from computer-assisted right lateral area measurement. Interrupted line shows the linear regression model correlating area of the right lateral projection with liver mass at autopsy. Solid lines show 95% confidence limits.

5. Manual dimension B (3). The diagonal measurement from the most superior extent of the dome to the most inferior part of the liver was used to approximate dimension B, which was originally reported to be a somewhat less effective index of liver disease than dimension A.

For each patient studied, the following computer-derived measurements were recorded:

6. Computer-assisted anterior area. The liver area was measured using the liver margins as defined from the anterior projection by the Laplacian operator.

7. Computer-assisted right lateral area. The liver area as seen from the right was similarly measured.

Manual measurements for index derivation were obtained by a single observer for each of the 50 patients in several sittings over a period of approximately 1 yr. The liver weight of each patient as found at autopsy was plotted against each of the manual and computer-assisted measurements tested, and generalized regression analysis was applied (6). Corresponding correlation coefficients and F-statistics were computed.

RESULTS

Liver weights found at autopsy in 50 patients were used to derive an index of liver mass, by representative methods that depend upon manual extraction of measurements from the liver images, and by computer-assisted area measurements of the

anterior and right lateral projections of the liver. The correlation coefficient between mass estimates and the liver weight at autopsy was also calculated for each method.

Figure 1 shows the data scatter and their correlation for the computer-assisted, right lateral area measurement. Figure 2 shows, for comparison, the same data when dimension A (longitudinal height of the liver) is used. Table 1 summarizes the correlation coefficients for each of the methods analyzed.

Liver-mass estimates derived from the computer-assisted right lateral area measurement showed the highest correlation with liver weight at autopsy, using the equation:

Liver Mass [kg] =
$$\text{Area } [cm^2]/275 \ [kg/cm^2] - 0.215 \ [kg]$$

We next studied several of the possible sources of the error. In order to determine whether the mass estimates were adversely affected by the delays between imaging and autopsy, the error in mass estimates from the best computer-assisted method was plotted against the interval between imaging and autopsy. As shown in Fig. 3, increasing delay between imaging and autopsy had little effect on error in the liver-mass estimate in this series of patients.

We performed experiments to estimate qualitatively potential observer error. The primary observer independently repeated all manual measurements on images from 26 patients over a few days. The correlation coefficient between the initial and
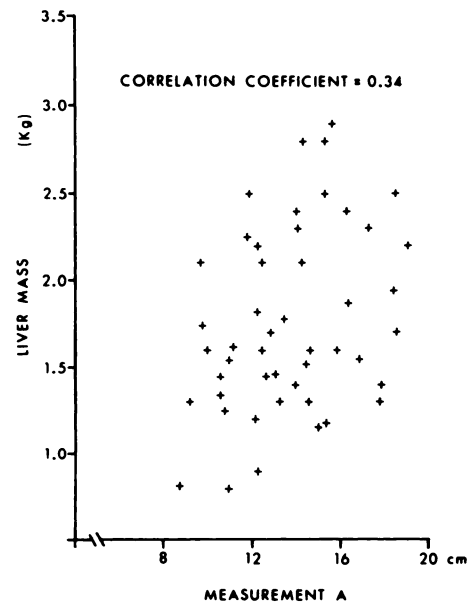

FIG. 2. Liver-mass index from manual measurement of dimension A (longitudinal height of liver).

146

TABLE 1. CORRELATION BETWEEN LIVER-MASS ESTIMATES AND LIVER WEIGHT AT AUTOPSY IN 50 SELECTED PATIENTS

Index method	Correlation coefficient
Manual, anterior area	0.49
Manual, right lateral area	0.65
Manual, geometric model	0.66
Manual, dimension A	0.33
Manual, dimension B	0.60
Computer, anterior area	0.61
Computer, right lateral area	0.83

TABLE 2. CORRELATION BETWEEN REPEATED LIVER-MASS ESTIMATES USING MANUAL LIVER-MASS INDICES

Manual method examined	Correlation coefficients	
	Single observer	Two observers
Anterior	.86	.89
Right lateral	.87	.89
Geometric model	.82	.86
Dimension A	.87	.83
Dimension B	.92	.87

repeat measurements in these patients was then calculated. Table 2 shows variation in single-observer measurement. To estimate variation between observers, a trained secondary observer independently extracted the liver measurements from the 26 patients in the same manner as the repeat measurements of the primary observer. The correlation between the second set of measurements by the primary observer and the measurements by the secondary observer was then calculated as shown in Table 2. The variation in measurement between observers appeared to be comparable to the variation in measurements by a single observer.

In order to study the manual methods' potential errors because of variations in imaging technique, image recordings from a separate series of 13 consecutive patients referred for liver images were manipulated to simulate plausible variations in imaging

FIG. 3. Lack of effect of time interval between liver imaging and autopsy on accuracy of liver-mass estimate by the computer-assisted right lateral area method.

technique. Three images of the anterior projection of the liver were obtained in each patient by using the approximate minimum, mean, and maximum gamma-camera intensity settings that produced a diagnostically acceptable gray scale within the image. Planimetry was used to measure the anterior area. The lowest acceptable intensity setting produced an area that averaged 11% lower than the area measured using the highest acceptable intensity.

DISCUSSION

The method we have developed for computer-assisted estimation of liver mass from the right lateral projection is more accurate and easier to apply than any of the adapted manual methods that we tested.

Our experiments to assess qualitatively observer variation and variations of imaging intensity setting show that these sources of error could appreciably contribute to the error we found using the manual methods. We conclude that the superiority of the computer-assisted method over the manual methods may be attributable in part to freedom from the effects of observer variation, and to freedom from the effect of changes in gamma-camera intensity setting. The computer-assisted method may underestimate the mass of livers with very large defects in radioactivity at the edge of the liver; we did not have such images in our series.

All of the methods tested, both manual and computer-assisted, are subject to additional error due to variations in organ orientation or shape, organ motion, or in patient positioning that may cause inconsistent projection for a particular liver mass.

The manual methods tested were originally described for use with rectilinear scan images. Our modifications to adapt the methods for use with the gamma camera introduced some potential sources of error not present with the original techniques. The full-sized images produced by most rectilinear
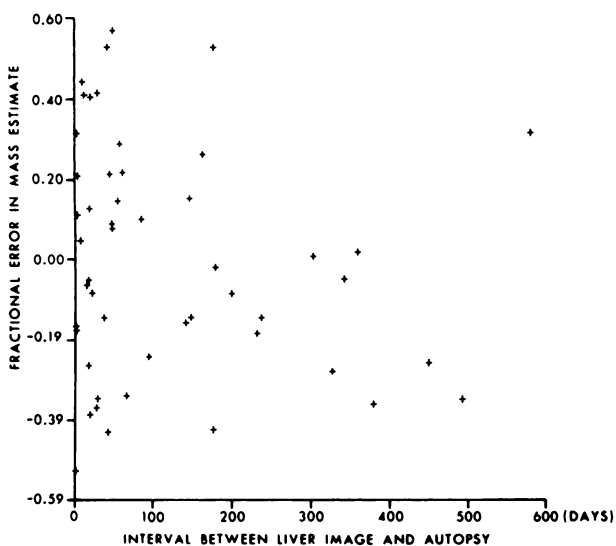
scanners may avoid the error introduced by optical enlargment of gamma-camera images for tracing. Focusing collimators used with rectilinear scanners produce a semitomographic image, which may make it easier to delineate the margins of the liver.

The authors who described the geometric model for estimation of liver mass reported on images from 15 patients from whom postmortem liver weights were available (2). Our calculations, using data from the original report, show a better than 0.99 correlation coefficient between calculated liver mass estimates and the liver weight found at autopsy. Observer error was also very low. The error we found in applying the method may be due in part to our adaptations necessary for using the method with the gamma camera.

Our results indicate that manual measurement of the anterior dimensions A and B (3), as adapted for use with the gamma camera, provided a poor basis for the estimation of liver mass. This finding does not necessarily contradict the original finding that these measurements could serve as predictors of liver disease (3).

We evaluated the right lateral projection in addition to the anterior projection because it gives more emphasis to the right lobe of the liver, which usually contributes more to liver mass than does the left lobe. This projection also is free from the ambiguity that may occasionally be caused by the spleen when it is included on the anterior projection. Patients were imaged supine because we thought this would result in the most reproducible right lateral projection.

Since liver mass is not always altered in liver diseases, the diagnostic value of liver-mass estimates may be highest when this feature is used in combination with other measureable image features such as liver-image texture (4, 5, 7). Liver-image features and other clinical data may then be assigned appropriate diagnostic weight by means of pattern recognition or other analytic techniques (8, 9). Further evaluation of computer-assisted liver-mass estimation from radiocolloid images is warranted in order to determine the value of this image feature as a predictor of liver disease in defined patient populations.

FOOTNOTES

* Pho/Gamma HP, Searle Radiographics, Des Plaines, IL.
† E. I. DuPont DeNemours Co., Wilmington, DE.
‡ Model 3352, Realist, Inc., Menomonee Falls, WI.

ACKNOWLEDGMENTS

REFERENCES

1. NAFTALIS J, LEEVY CM: Clinical estimation of liver size. Am J Dig Dis 8: 236–243, 1963
2. ROLLO FD, DELAND FH: The determination of liver mass from radionuclide images. Radiology 91: 1191–1194, 1968
3. ROSENFIELD AT, SCHNEIDER PB: Rapid evaluation of hepatic size on radioisotope scan. J Nucl Med 15: 237–240, 1974
4. JAIN VK, EIKMAN EA, FLOWER D, et al: A method for computer analysis of texture in radionuclide liver images. Proceedings of the 15th Annual San Diego Biomedical Symposium Vol 14: 167–173, 1975
5. EIKMAN EA, JAIN VK, MADDEN JA, et al: A texture vector approach to detect focal defects in radionuclide liver images. Proceedings of the 15th Annual Meeting of San Diego Biomedical Symposium, Vol 15: 203–206, 1976
6. DRAPER N, SMITH H: Applied Regression Analysis. John Wiley & Sons, Inc., New York, 1966, pp. 335–342
7. MACK GA, JAIN VK, MADDEN J, et al: Polar reference texture in radiocolloid liver images. Proceedings of the 1978 IEEE Computer Society Conference on Pattern Recognition and Image Processing, pp. 369–371, 1978
8. MADDEN JA, JAIN VK, MACK GA, et al: Development of a fortran pattern recognition system for a minicomputer. Proceedings of the Sixth Symposium on the Sharing of Computer Programs and Technology in Nuclear Medicine, pp. 378–384, 1976
9. JAIN VK, MADDEN JA, MACK GA, et al: Directed CLAFIC: An entropy-based method for feature compression. Proceedings of the San Diego Biomedical Symposium Vol 17: 163–168, 1978